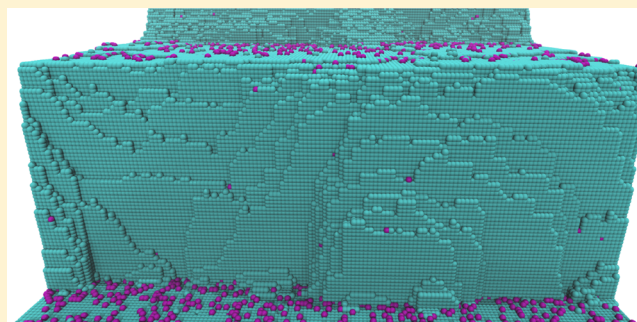


Mineral Growth beyond the Limits of Impurity Poisoning

Mike Sleutel,^{*,†} Jim Lutsko,[‡] and Alexander E. S. Van Driessche[§][†]Structural Biology Brussels, Vrije Universiteit Brussel, Pleinlaan 2, 1050, Brussels, Belgium[‡]Center for Nonlinear Phenomena and Complex Systems, Code Postal 231, Université Libre de Bruxelles, Boulevard du Triomphe, 1050 Brussels, Belgium[§]Université Grenoble Alpes, CNRS, ISTERre, F-38000 Grenoble, France

Supporting Information

ABSTRACT: More often than not, minerals formed in nature are grown at low supersaturation and from sources that are impure with respect to the crystals' main building blocks. Quite paradoxically, these conditions are in conflict with the established crystal growth theories that focus on the interplay between the crystal interface and impurities that are present in the growth medium. These theories predict a kinetic *dead zone* for the cases where low purity is combined with weak driving forces. Hints toward reconciling this apparent disparity have been given by the observation that a specific class of steps, so-called macrosteps, can circumvent the debilitating kinetic effects of impurities in ways that up until now are poorly understood. In this contribution, we examine the mechanism of crystal growth by means of kinetic Monte Carlo simulation at conditions close to impurity-induced kinetic arrest. In agreement with previous reports, we show that as a result of impurity binding to the crystal surface, steps spontaneously group into bunches and later condense into macrosteps. A kinetic analysis demonstrates that these macrosteps are able to evade crystal growth cessation under conditions where single steps are firmly pinned. We identify the mechanism of interstep cooperativity which leads to *cessation evasion* by macrosteps and demonstrate that it applies to a range of supersaturation and impurity concentration values. On the basis of these findings, we present a model that explains how minerals can grow from mother liquor solutions that would otherwise seem to be nonconductive to crystal growth.



INTRODUCTION

Scientists working in the fields of mineralogy, geochemistry, and biomineralization are faced with an apparent contradiction: solution grown natural minerals are formed under conditions that are in conflict with the existing models of crystal growth. Natural minerals are frequently formed at low supersaturation from heterogeneous solutions. Some typical examples include the gradual formation of (non)marine evaporites in slowly shrinking bodies of water,¹ the development of Ca and Mg scalants on reverse osmosis membranes and in heat-exchange units,² or the formation of kidney or gallstones in vivo.³ Probably the most spectacular example is the giant gypsum crystals discovered at the beginning of this century in the Naica Mine, Mexico.^{4,5} Chemical analysis of the Naica aquifer has revealed that known impellers of gypsum growth are present at concentrations as high as 5 mM or up to 30% of the Ca concentration (e.g., Mg, K, Na).^{6,7}

These examples correspond to crystallization environments that differ substantially from pristine laboratory conditions in that the presence of species distinct from the main crystal constituents is likely to be the rule rather than the exception. Conditions that combine a weak driving force for crystallization with a low purity of the main solute are the leading cause of crystal growth cessation before equilibrium has been reached, at

least this is the prediction of established crystal growth theories.^{8–10} Such theories focus on the interaction of unfinished crystal layers (steps of unit height) and foreign species that adsorb to the crystal–liquid interface. The latter are *imperfect imposters* of the main solute in that they partially replicate the interatomic bonding of the crystal along one direction, but drastically alter it in another.

Impurities that adsorb to crystal facets can completely inhibit the growth of a crystal under supersaturated conditions.^{11,12} The range of nonzero supersaturations where such premature kinetic arrest occurs is referred to as the width of the dead zone (σ_d). There have been a number of theoretical efforts to make quantitative predictions of σ_d leading to a multitude of expressions, but the common denominator is that a critical density of firmly adsorbed impurities is required to halt the progression of steps.^{13–15} Those predictions are defied by the observations for a number of systems^{16,17} which exhibit clear growth within the reported dead zone. A key observation is that growth in such cases is mediated by groups of closely spaced steps, so-called step bunches or in the limit of a vanishing

Received: July 31, 2017

Revised: November 22, 2017

Published: December 4, 2017

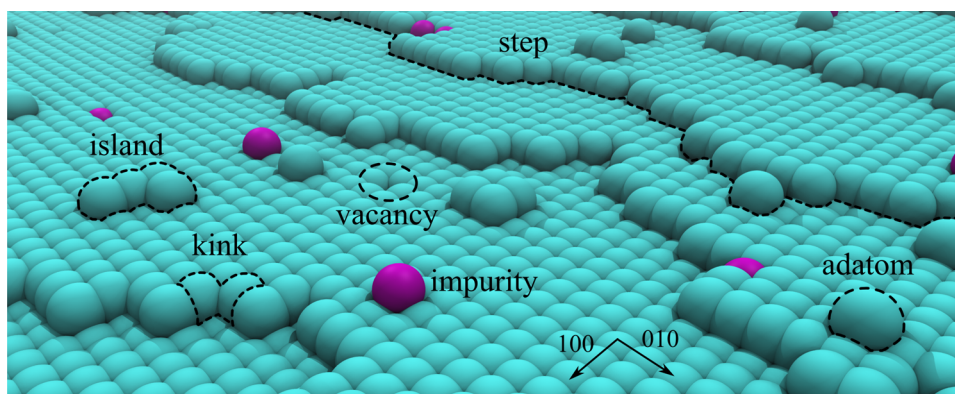


Figure 1. Atomic rendition of the solid-on-solid model used in our kMC setup: we follow the dynamics of a vicinal (001) Kossel face by allowing the following elementary actions: adsorption and desorption of adatoms and impurity atoms, lateral diffusion of adatoms over terraces and across steps, attachment to and detachment from step edges and kinks. Equilibrated surfaces below the roughening temperature exhibit the classical features of a crystal surface, i.e., terraces, vacancies, adatoms, and 2D clusters.

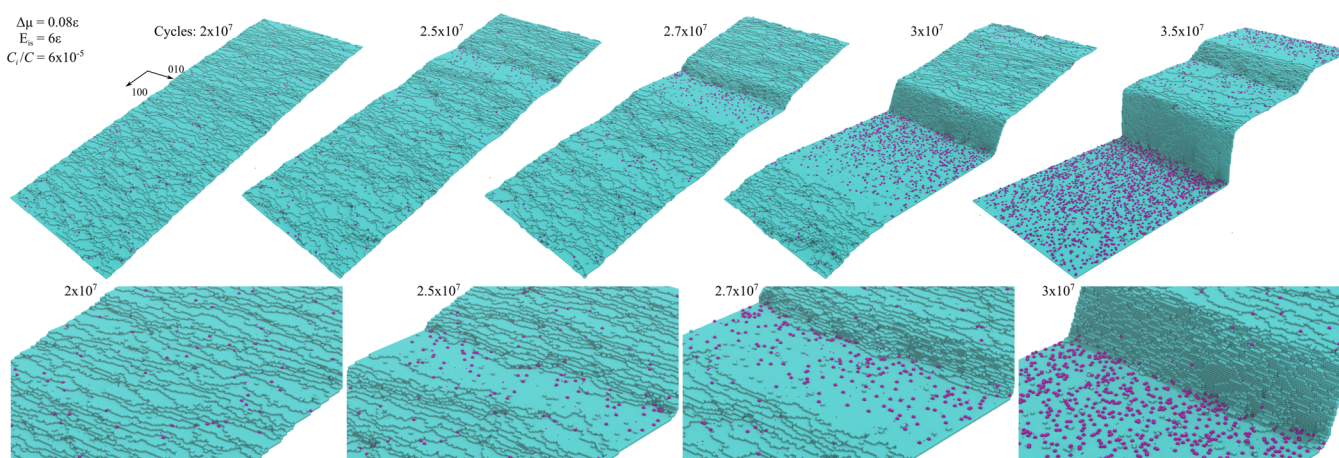


Figure 2. Dynamic coarsening of a vicinal (001) Kossel surface with no Schwoebel barrier: we start from an impurity free equidistant step train and follow its evolution over time at $\Delta\mu = 0.08\epsilon$, $E_{is} = 6\epsilon$, and $C_i/C = 6 \times 10^{-5}$. Step density fluctuations translate into a temporary increase of the terrace exposure time resulting in local increase of impurity adsorption. This triggers a step bunching cascade that ultimately leads to macrostep formation.

interstep distance, macrosteps. Macrostep growth within the dead zone conflicts with the intuitive view that the velocity of a macrostep is limited by the rate of advance of the bottom step, which is assumed to be either identical or smaller than that of an isolated step.¹⁸ This anomalous behavior implies that macrosteps interact differently with surface bound impurities in a way that is currently unknown, but which results in a net nonzero growth rate of the crystal under conditions where isolated steps would otherwise remain fixed. The missing physics not only defies our fundamental understanding of crystal growth, but could also be used to guide the future development of tailor-made impurities that could serve as antiscalants in desalination plants, or could help prevent stone formation *in vivo*.

As of yet, the interaction of macrosteps with impurities has remained largely unresolved mainly due to experimental limitations. Even state-of-the-art imaging techniques lack the ability to resolve the steps that make up a macrostep and the surface bound impurities that interact with it. In order to make progress on the issue, we performed kinetic Monte Carlo (kMC) simulations using a solid-on-solid scheme by which we can inspect the system at the required atomic level (Figure 1). Our methodology is complementary to more coarse-grained semimicroscopic models that have been successfully employed

to describe the coarsening behavior at long time scales and the emergence of steady states.^{19–24} Of particular relevance is the work by Ranganathan and Weeks^{23,25} who have used a terrace-step-kink model to investigate the growth recovery of pinned steps. Their model elegantly captures the general experimental trends but does not provide a detailed view on the physics of step cooperativity at the nanoscopic scale discussed above.

In previous contributions, we presented our basic kMC framework and benchmarked it first for single steps,^{26,27} and subsequently macrosteps.²⁸ Our work on macrosteps was limited to fairly artificial models in which the dynamics of the problem—the formation of macrosteps and the dynamic attachment and detachment of impurities—was ignored. We also ignored the roles of supersaturation and impurity concentration which are critical to the problem at hand and are the main focus of this work. Furthermore, we find a crucial connection between fluctuations in impurity adsorption densities and the formation of macrosteps which is not accessible to models with static impurities.

Using the revised kMC framework presented below, we have performed an in-depth analysis of the kinetics of macrostep formation and growth in the presence of dynamic impurities, and compare it to the kinetic response of single steps. From the simulations, we identify the mechanism of interstep coopera-

tivity which leads to *cessation evasion* by macrosteps and demonstrate that it applies to a broad range of supersaturation and impurity concentrations. Finally, we present a model that explains how minerals can grow from mother liquor solutions that are currently deemed to be uncondusive to crystal growth.

RESULTS

Initiation of Bunching of Steps into Macrosteps. We start out with fully equilibrated step trains in the absence of impurities and show that subsequent exposure of vicinal surfaces to impurities at a concentration of C_i induces spontaneous bunching of steps into macrosteps (Figure 2). The latter requires that impurities are fully dynamic, by allowing adsorption and desorption to occur randomly, leading to nonequilibrium concentrations of the adsorbed impurities. We apply a strong downward vertical bonding (E_{is}) between the impurities and the solute, which leads to impurities that are able to pin steps by preferentially populating the terraces in between the steps.

We first work in the high-kink density limit by setting the temperature sufficiently high relative to the bond energy. This is the usual limit in most step pinning theories where steps are viewed as linear sinks with respect to the solute and considered to be flexible enough to bend round fixed impurities that are bound to the surface. Such flexibility leads to a constantly changing microscopic roughness at finite temperatures, and steps meander by consequence. Step meandering leads to an effective entropic repulsion between steps that is poorly understood at the quantitative level, but of particular relevance for regions of the crystal surface with high step density. Rather than imposing entropic repulsion in an *ad hoc* manner by using an effective step–step interaction potential, it is a natural consequence from the atomic-level description of our system.

The panels of Figure 2 show the evolution of the crystal topography as a function of time for conditions of low supersaturation and a concentration of impurities in solution which is 6×10^{-5} times that of the growth species. The system starts out as an equidistant step train that can be characterized by a mean rate of advance. Local fluctuations in the rate of step advancement, however, translate into variations of the local terrace width. Larger terraces are characterized by longer exposure times and are therefore more susceptible to impurity binding. Over time, this induces the formation of local impurity hot spots that can trigger a step bunching cascade leading to the spontaneous formation of macrosteps. We did not find a stable step bunch size: after a sufficient long simulation time, all steps become grouped into a single step bunch. In certain limits which we will discuss below, such a step bunch can become gradually compressed and eventually transforms into a macrostep that corresponds in structure to the (100) facet.

Macrostep Growth within the Dead Zone of Single Steps. Having established that impurity induced step bunching occurs spontaneously in our system, we proceed by performing a kinetic analysis of the macrostep motion across impurity poisoned terraces. To obtain reliable estimates of steady state macrostep velocities, we work with surfaces that are equilibrated with respect to the impurity density on the terraces. By allowing the impurity adsorption/desorption processes to fully relax, we can precisely control the impurity concentration n_i on the surface by changing the concentration of impurities in solution, C_i . The goal here is to mimic conditions close to kinetic arrest, well after bunching has taken place, where we assume that maximal impurity coverage has

been reached for the chosen C_i . Taking such poisoned facets as a starting point, we populate the surface with either a macrostep composed of 20 steps, or a single elementary step, and monitor the average change of mass as a function of time (dM/dt), normalized for the total mass of steps on the surface and the dimension of the simulation cell in the [010] direction. For conditions where two-dimensional (2D) nucleation can be neglected, dM/dt serves as a good approximation of the rate of advance v of a step (see Supporting Figure 1). The choice to work with macrosteps composed of 20 elementary steps is based on previous work²⁸ where we have shown that the rate of macrostep advancement through a field of impurities is dependent on the height of the macrostep. That dependence saturates for macrosteps of 10 steps or larger. The macrostep size in this work represents a compromise between maximizing the number of constituent elementary steps while still keeping the size of the simulation cell within workable dimensions (with respect to the required computing resources).

Figure 3 shows the dependence of the steady-state step front velocity v as a function of supersaturation for a range of n_i values, for a single elementary step (Figure 3a), and for a macrostep of height 20 (Figure 3b), respectively. For a single step, v is zero within the error bars below a critical

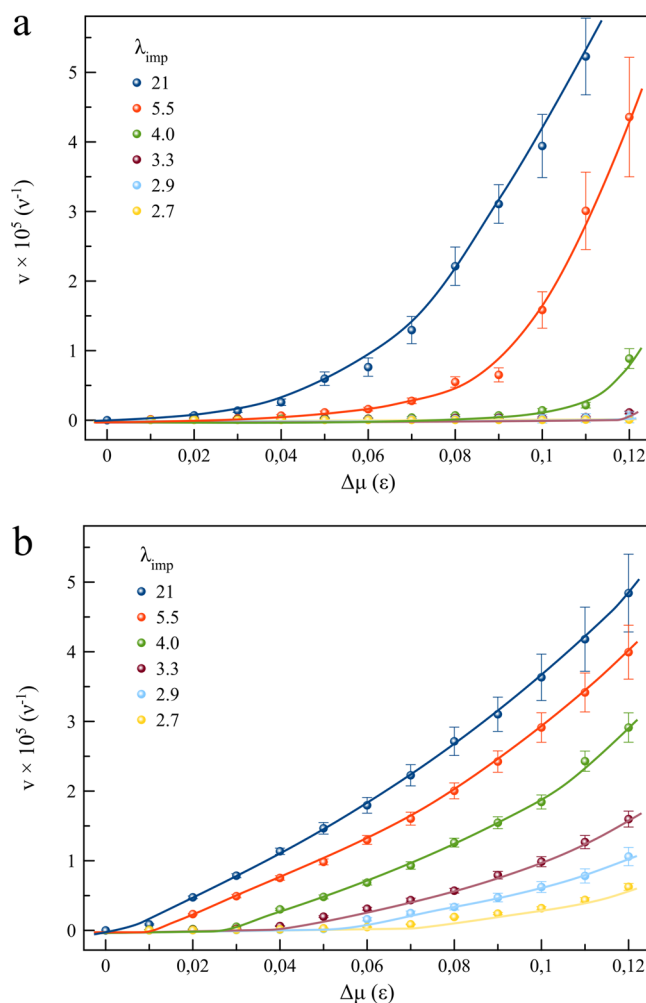


Figure 3. Steady-state step front velocity v as a function of supersaturation for a range of C_i values: (a) single steps, (b) macrosteps composed of height 20; the corresponding interimpurity distance λ_{imp} on the (001) surface is indicated in the legend.

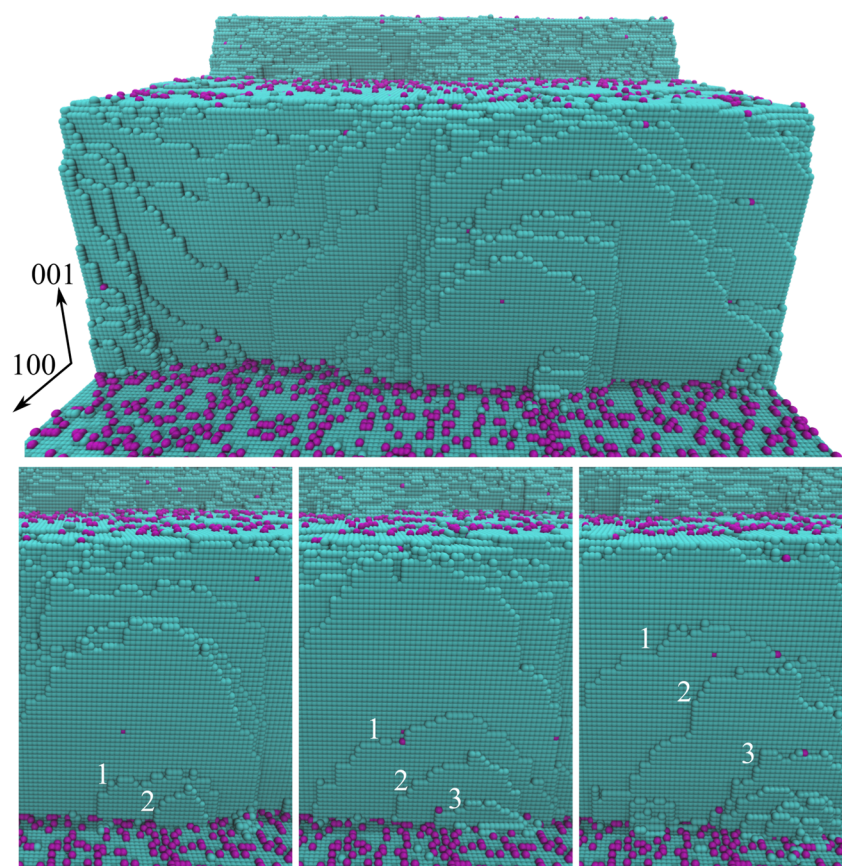


Figure 4. Mechanism of macrostep growth through an impurity field: macrosteps bypass the blocking effect of a row of impurities by allowing single steps to grow in the out-of-plane [001], rather than the in-plane [100] direction. Three steps breaking through the impurity fence are highlighted in the three bottom panels to illustrate the layer-by-layer growth leading to a net advancement of the macrostep in the [001] direction (see [Supporting Video](#)).

supersaturation and exhibits a sharp monotonic increase for $\Delta\mu$ larger than σ_d^{single} . This is in complete agreement with experimental observations and corresponds to the existence of a dead-zone. The same qualitative result is obtained for macrosteps, but the width of the dead zone σ_d^{macro} is significantly reduced. The fact that $\sigma_d^{\text{macro}} \ll \sigma_d^{\text{single}}$ for all the tested n_i demonstrates that macrostep growth is possible under conditions where single steps are otherwise fixed. Crystal surfaces that are solely populated with single steps are therefore more susceptible to premature kinetic arrest induced by impurities than if macrosteps would be present. This then raises the question: how do macrosteps manage to advance under impure conditions where single steps remain firmly pinned?

Mechanism of Macrostep Growth on Impurity Poisoned Surfaces. To answer that question, we render the molecular snapshots of the simulation and look at the atomic structure of a macrostep advancing through a field by impurities (Figure 4). The macrostep shown in Figure 4 can be considered as a local realization of a (100) facet. Advancement of this facet occurs in a layer-by-layer fashion in the direction normal to the impurity poisoned (001) surface. More precisely, single steps break through the impurity fence at the intersection of the (001) and (100) faces, and grow quasi unperturbed in the [001] direction on the (100) facet which is devoid of impurities. One can see why the piercing of steps through the impurity fence in the *vertical* direction is possible, even when it is not in the *horizontal* direction, by considering the typical step

pinning scheme that was argued by Cabrera and Vermilyea, i.e., a grid of impurities blocking an elementary step. Because we are working at conditions that are within the dead zone of single steps, the typical distance between impurity atoms is on the same order as the critical size of a step protuberance piercing the space between two impurities. It is therefore likely that such a protrusion will encounter other impurities before it reaches supercritical dimensions. This creates an additional barrier for further growth which does not exist for steps moving in the [001] direction.

For step motion to be possible in the [001] direction, step bunches need to be compressed into faceted macrosteps. The latter entails that steps are linearized into their fully extended form, and the process is therefore likely to be associated with an entropic cost. This is exemplified by the equilibration of a single macrostep of height 20 at zero supersaturation with no impurities present. The simulated macrostep spontaneously decays into an equidistant step train in the absence of a compressing force. We monitor the enthalpy of the system normalized for the total number of simulated atoms and record a monotonic increase as a function of time of about 10% as the system evolves from a macrostep to a step train (Figure 5a). The enthalpy increase stems from the increase of the total number of dangling bonds due to the formation of kinks as steps gradually roughen and is offset by a corresponding increase in entropy.

The associated entropic cost for the reverse process—transformation of a step train into a macrostep—can be

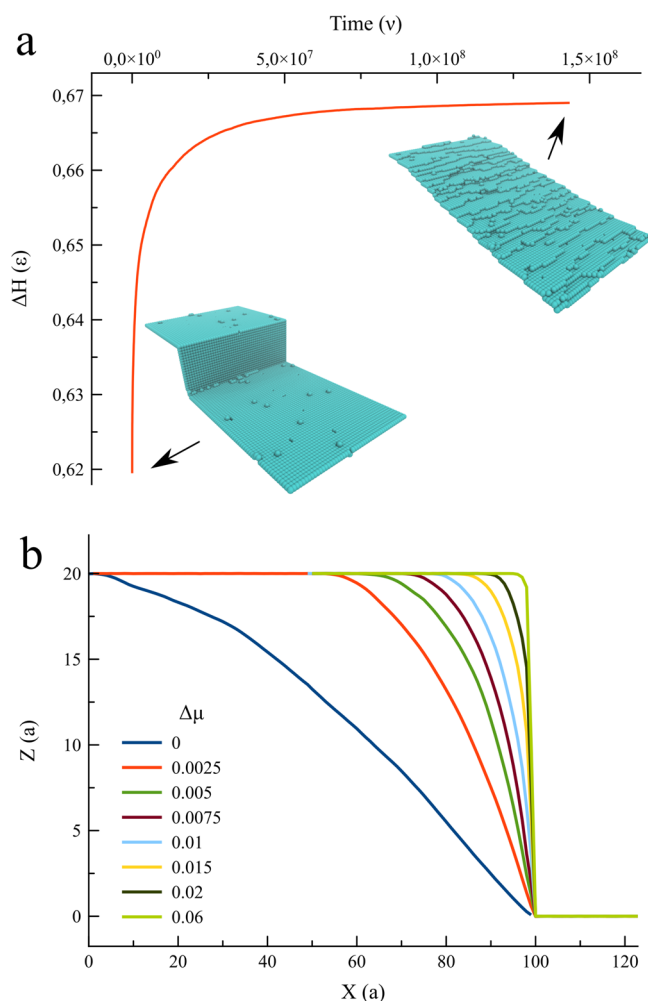


Figure 5. (a) Macrostep decay in the absence of impurities at equilibrium: enthalpy ΔH evolution as a function of time; (b) macrostep relaxation as a function of supersaturation with the bottom step pinned by a line of impurities at $X = 100a$: Steady-state macrostep structure as a function of $\Delta\mu$. X and Z correspond to the lattice coordinates along the $[010]$ and $[001]$ direction, respectively.

compensated by increasing the enthalpic gain by raising the supersaturation. This is illustrated by a series of simulation runs performed on a step bunch which is being pinned by a line of impurities at its leading end. In Figure 5b we plot the time-averaged projection of the macrostep profile along the $[010]$ direction for a range of supersaturation values. We observe a gradual transformation from a step train into a fully compressed macrostep by increasing $\Delta\mu$ from 0ϵ to 0.05ϵ . Even a value as low as 0.015ϵ suffices to reach partial compression of the macrostep, with the bottom 10 steps already forming a local (100) facet. The contribution of entropic repulsion to macrostep destabilization becomes even weaker for steps with lower kink densities. Indeed, by keeping $\Delta\mu$ constant and gradually decreasing kT we can tune the kink density. These simulations demonstrate that step trains are more easily compressed into macrosteps at lower kT (lower kink density), in line with the prediction for the entropic repulsion (data not shown).

Diffusion-Limited Kinetics. So far we did not explicitly model the fluid that is in contact with the crystal interface. This approach essentially corresponds to working in the regime where crystal growth is limited by the kinetics of incorporation.

In this limit, solute transport by diffusion to the kinks is fast with respect to the rate of incorporation, and solute depletion effects can be ignored. However, crystal growth can also be under mixed or kinetics control, where non-negligible solute depletion will occur. To incorporate that additional level of complexity, we adapt our kMC scheme to explicitly model the solute molecules in the fluid as well and therefore allow for gradients to be formed. This is implemented by fixing the inward flux of solute and impurity atoms into the n th fluid layer above the crystal surface, and controlling the rates of diffusion D_s and D_i within that volume. This method is inspired by the generally accepted notion of the existence of a diffusive layer close to the crystal–fluid interface where mass transport is limited to diffusion and outside of which C_s and C_i reach their bulk values.¹⁸

Using this explicit-fluid kMC scheme we find that the average solute density C_s within the i th fluid layer increases linearly as a function of the distance normal to the crystal surface for a range of $\Delta\mu$ and D_s values. This demonstrates that for the chosen conditions, we are indeed operating in the diffusion-limited regime. We now follow the dynamic coarsening of a step train that is initially devoid of impurities, but becomes gradually poisoned as we set $C_{i,n}/C_{s,n}$ from 0 to 0.001 (Figure 6a). The result is qualitatively similar to the step bunching observed under kinetics control in that macrosteps form spontaneously after a sufficient long simulation time (e.g., 6.2×10^7 kMC cycles).

It is interesting to note that the mechanism of impurity uptake into the crystal changes as the surface gradually coarsens from a step train into a step bunch, and in the limit a macrostep. This is exemplified in Figure 6b where we render the impurity atoms within the volume of a crystal that has undergone such a coarsening transition. The resulting picture shows a gradual evolution from a homogeneous impurity distribution (bottom region) to the emergence of impurity-rich bands (upper region). Impurity banding is a well-known crystal growth phenomenon and has been assumed to be related to step bunching, but remains challenging to characterize at a microscopic level. Our simulation snapshots clearly show that impurity densities are highest in the crystal layers that are formed by the leading, bottom step of a macrostep, followed by a drastic decrease of impurity density for the remaining layers of the macrostep. We point out that the regular spacing between the impurity bands is the result of the boundary conditions used in our simulations and is in that sense specific for the simulation settings. For larger systems with macrosteps of various heights, banding will still be present but is expected to be less regular.

DISCUSSION

Our data on the growth of vicinal surfaces close to kinetic arrest match the earlier experimental observations for potassium dihydrogen phosphate crystals poisoned by Fe^{3+} ,^{16,17} and the more recent observations for diamond crystals as-grown in Mg-based systems.²⁹ The kinetic differences between surfaces populated solely with elementary steps or with macrosteps are striking. Both experiment and simulation have demonstrated that crystals can grow under conditions that were previously thought to be nonconducive for crystal growth. Despite those observations, it has remained largely unknown how macrosteps manage to postpone premature cessation of growth. The atomistic picture for the Kossel system studied here provides a clear answer to that question. The key point is that step

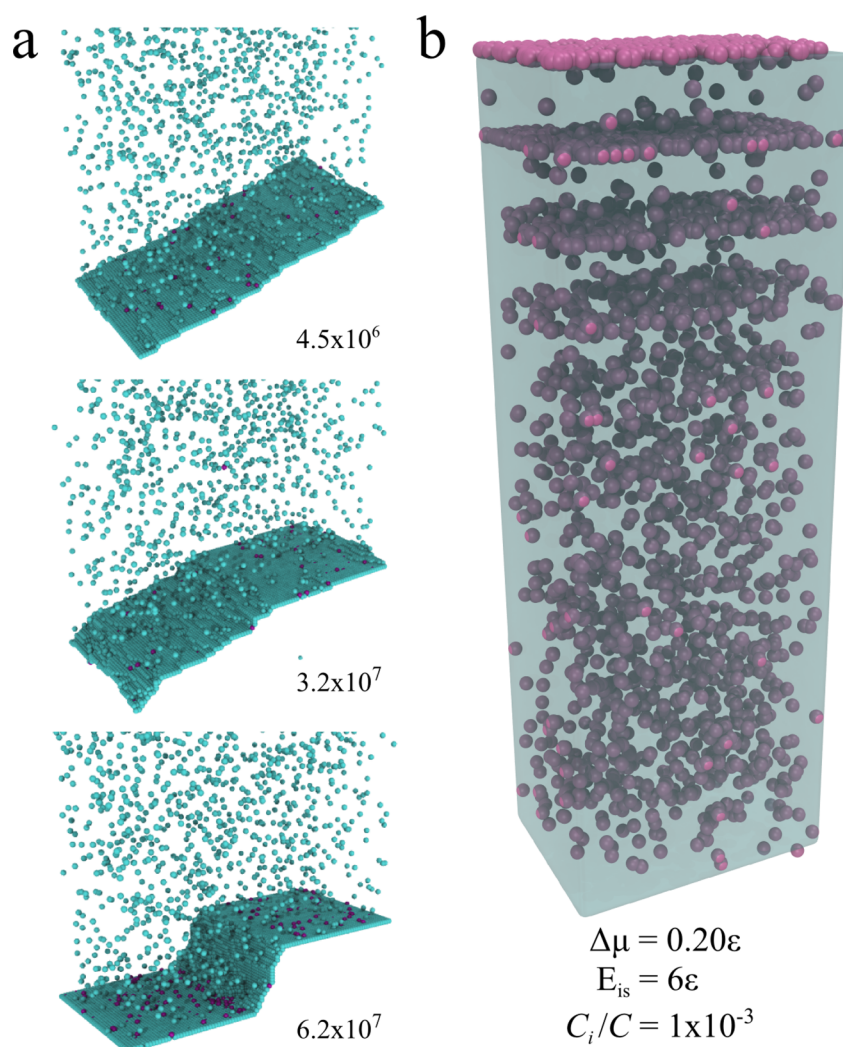


Figure 6. Explicit fluid kMC simulations: (a) dynamic coarsening of a step train exposed to a fluid layer of height 200 with $C_{i,n}/C_{s,n} = 10^{-3}$ and $\Delta\mu_n = 0.2\epsilon$. The number in the lower right denotes the number of kMC cycles; (b) distribution of impurity atoms (pink) within the crystal volume (shaded blue) of the crystal in (a).

bunches become compressed into macrosteps with vanishing interstep distances under a broad range of pinning conditions. Interestingly, step bunching is induced in the regime close to kinetic arrest. One can view this as a kinetic response mechanism of the crystal that seems contradictory at first. Namely, grouping of steps into bunches yields large terraces with long exposure times, which enhances the impurity effects on single steps. Although it leads to a global reduction of the crystallization rate, it also triggers the formation of macrosteps that are able to bypass the most *crippling* impurity effects and continue to move even when single steps are firmly pinned by terrace bound stoppers. This is precisely the point. The difference with a low, but finite growth rate (macrosteps) and complete kinetic arrest (single steps) can have a large impact on the total crystallized volume at long time scales, such as those found for the giant gypsum crystals of Naica, where crystal growth took place over 1 Ma, at a very slow, but steady rate.⁵

■ EXPERIMENTAL SECTION

Kinetic Monte Carlo Simulation Method. Our simulations use a standard kinetic Monte Carlo (kMC) method with fixed time step commonly referred to as a solid-on-solid (SOS) model in 2 + 1

dimensions. The simulation geometry consists of some fixed number of cells in the x - and y -directions, N_x and N_y , respectively, and an arbitrary number of cells in the positive z -direction. One Monte Carlo move consists of $N_x N_y$ individual updates of the surface. Each individual update consists of randomly choosing one of the surface molecules and randomly choosing a primitive action to execute. The primitive actions are to (a) adsorb a new crystal molecule, (b) adsorb an impurity molecule, (c) desorb the existing surface molecule, and (d) randomly move the existing surface molecule in one of the four possible directions. The probability of each primitive action is computed as $\tau\nu_i e^{-E_i/k_B T}$, where ν_i is the attempt frequency for the i th action, E_i is the energy barrier for that action and τ is the time step, which is set to $(\sum \nu_i \max(e^{-E_i/k_B T}))^{-1}$, the sum being over all primitive actions and the $\max()$ function, indicating that we take the minimum possible value of the energy barrier. In general, we take the energy barriers to be the sum of the energies of the bonds that are broken during the primitive action or the chemical potential for actions involving adsorption of a molecule from solution. We used periodic boundary conditions in the x - and y -directions: the nearest neighbor in the x -direction for the cell at (N_x, y, z) is $(1, y, z)$ and vice versa. For the boundary in the direction of step growth, the periodicity is combined with a shift in the vertical direction to allow steps to cross the boundary unimpeded. Extensive details can be found in ref 26.

Kinetic Monte Carlo Simulation Method with Explicit Fluid. To generalize the kMC model to include an explicit representation of

the fluid, we extend the lattice into the perpendicular (z) direction a number of layers, N_z . Instead of molecules appearing randomly on the surface of the crystal at a rate proportional to $e^{\beta\mu}$ as in the SOS model, they enter the surface at the upper boundary at this rate. This has the effect of giving a boundary condition of fixed chemical potential at the upper surface. Otherwise, molecules that are not attached to the surface perform a random walk with some hopping rate, ν_{liq} . These molecules do not interact with one another except for the requirement that each lattice site be singly occupied: if a molecule tries to hop onto an already-occupied site, the move is rejected. Otherwise, the dynamics consists of the obvious extension of the SOS model with two subtleties.

The first subtlety has to do with the boundary conditions. In the SOS model, when simulating elementary steps, the periodic boundaries in the direction of step propagation are displaced so that if the step is parallel to the y -axis and propagates in the x -direction, then the neighbor of a molecule with coordinates $(0, y, z)$ is $(N_x - 1, y, z + 1)$. When simulating macrosteps (or multistep trains) consisting of n steps, the displacement in the z -direction is n units when crossing the boundary. This simple trick allows steps to propagate smoothly across the periodic boundary. For the explicit fluid, a molecule leaves the simulation volume when it is at position $(x, y, N_z - 1)$ and makes a move in the positive z -direction. With the displaced boundary conditions, it will also leave the simulation volume when it is at $(N_x, y, N_z - 1)$ and attempts a move in the x -direction since this will send it to $(N_x + 1, y, N_z - 1)$ and (via action of the displaced periodic boundaries) to $(0, y, N_z)$ which is therefore outside the simulation volume. In order to preserve detailed balance (a critical requirement to have a kMC scheme that produces an equilibrium state), we must therefore allow molecules to enter the simulation volume not only at the positions $(x, y, N_z - 1)$ but also at $(N_x, y, N_z - 2), \dots, (N_x, y, N_z - n)$.

The second subtlety concerns the algorithm for attachment of a liquid molecule to the solid. The obvious criterion might be that if the lattice site (x, y, z) is occupied, then a liquid molecule that hops to the site $(x, y, z + 1)$ would automatically attach to the crystal. However, this leads to potential complications. For example, if a (second) liquid molecule was already at position $(x, y, z + 2)$, then when the first one hopped to $(x, y, z + 1)$ and attached, then should the one above it at $z + 2$ also attach? If it does, then we must account for a kind of two-particle move, which adds complication. In particular, detailed balance (which requires that all moves be reversible) would require that we allow for the detachment of pairs of molecules from the crystal. If we avoid these complications by not attaching the second molecule, then we have another problem with detailed balance. For the next move could be that the second molecule moves from $(x, y, z + 2)$ to $(x, y, z + 3)$, but now, this move is not reversible. For if it tries to hop back to position $z + 2$ it will automatically attach to the crystal, and we do not recover the original state (i.e., with the molecule in the site at $z + 2$ but not attached). For these reasons, we make attachment a separate event. This means that if the first molecule hops to site $(x, y, z + 1)$, it does not attach to the solid. It will only attach if it attempts a subsequent move that would send it to site (x, y, z) . When this move is attempted, the molecule attaches. Similarly, in keeping with detailed balance, when a molecule detaches from the solid it is not displaced: it remains in the same position but enters the liquid (which means that in subsequent moves it can make diffusive hops or reattach to the crystal). In this way, detailed balance is preserved in all cases, and we avoid the complexity of multiparticle moves.

■ ASSOCIATED CONTENT

Supporting Information

The Supporting Information is available free of charge on the ACS Publications website at DOI: 10.1021/acs.cgd.7b01057.

Supporting Figure 1 (PDF)

Supporting Video 1 (AVI)

■ AUTHOR INFORMATION

Corresponding Author

*E-mail: mike.sleutel@vub.be.

ORCID

Mike Sleutel: 0000-0003-3247-2187

Notes

The authors declare no competing financial interest.

■ ACKNOWLEDGMENTS

M.S. acknowledges financial support by the FWO under Project G0H5316N. The work of J.F.L. was supported by the European Space Agency under Contract Number ESA AO-2004-070.

■ REFERENCES

- (1) Warren, J. K. Evaporites through time: Tectonic, climatic and eustatic controls in marine and nonmarine deposits. *Earth-Sci. Rev.* **2010**, *98*, 217–268.
- (2) Sheikholeslami, R. *Fouling in Membranes and Thermal Units: A Unified Approach - Its Principles, Assessment, Control and Mitigation*, Balaban Desalinations, 2007.
- (3) Chung, J.; Granja, I.; Taylor, M. G.; Mpourmpakis, G.; Asplin, J. R.; Rimer, J. D. Molecular modifiers reveal a mechanism of pathological crystal growth inhibition. *Nature* **2016**, *536*, 446–450.
- (4) García-Ruiz, J. M.; Villasuso, R.; Ayora, C.; Canals, A.; Otálora, F. Formation of natural gypsum megacrystals in Naica, Mexico. *Geology* **2007**, *35*, 327–330.
- (5) Van Driessche, A. E. S.; García-Ruiz, J. M.; Tsukamoto, K.; Patiño-Lopez, L. D.; Satoh, H. Ultraslow growth rates of giant gypsum crystals. *Proc. Natl. Acad. Sci. U. S. A.* **2011**, *108*, 15721–15726.
- (6) Hamdona, S.; Nessim, R.; Hamza, S. Spontaneous precipitation of calcium sulphate dihydrate in the presence of some metal ions. *Desalination* **1993**, *94*, 69–80.
- (7) Hamdona, S. K.; Al Hadad, U. A. Crystallization of calcium sulfate dihydrate in the presence of some metal ions. *J. Cryst. Growth* **2007**, *299*, 146–151.
- (8) Cabrera, N.; Vermilyea, D. A. *Growth and Perfection of Crystals*; Doremus, R., Roperts, B., Turnbull, D., Eds.; Wiley: New York, 1958; pp 393–410.
- (9) Bliznakow, B. Die Kristalltracht und die Adsorption fremder Beimischungen. *Fortschr. Min.* **1958**, 149–191.
- (10) Sangwal, K. Effects of impurities on crystal growth processes. *Prog. Cryst. Growth Charact. Mater.* **1996**, *32*, 3–43.
- (11) De Yoreo, J. J.; Vekilov, P. G. Principles of Crystal Nucleation and Growth. *Rev. Mineral. Geochem.* **2003**, *54*, 57–93.
- (12) van Enkevort, W. J. P.; Los, J. H. Tailor-Made Inhibitors in Crystal Growth: A Monte Carlo Simulation Study. *J. Phys. Chem. C* **2008**, *112*, 6380–6389.
- (13) Kubota, N.; Mullin, J. A kinetic model for crystal growth from aqueous solution in the presence of impurity. *J. Cryst. Growth* **1995**, *152*, 203–208.
- (14) Weaver, M. L.; Qiu, S. R.; Hoyer, J. R.; Casey, W. H.; Nancollas, G. H.; De Yoreo, J. J. Improved Model for Inhibition of Pathological Mineralization Based on Citrate Calcium Oxalate Monohydrate Interaction. *ChemPhysChem* **2006**, *7*, 2081–2084.
- (15) Potapenko, S. Y. Threshold for step percolation through impurity fence. *J. Cryst. Growth* **1993**, *133*, 141–146.
- (16) Land, T. A.; Martin, T. L.; Potapenko, S.; Palmore, G. T.; De Yoreo, J. J. Recovery of surfaces from impurity poisoning during crystal growth. *Nature* **1999**, *399*, 442–445.
- (17) Ristic, R. I.; DeYoreo, J. J.; Chew, C. M. Does impurity-induced step-bunching invalidate key assumptions of the Cabrera-Vermilyea model? *Cryst. Growth Des.* **2008**, *8*, 1119–1122.
- (18) Chernov, A. A. *Modern Crystallography III. Crystal Growth*; Springer-Verlag: Berlin, 1984.
- (19) van der Eerden, J. P.; Muller-Krumbhaar, H. Dynamic Coarsening of Crystal Surfaces by Formation of Macrosteps. *Phys. Rev. Lett.* **1986**, *57*, 2431–2433.

(20) Kandel, D.; Weeks, J. D. Theory of impurity-induced step bunching. *Phys. Rev. B: Condens. Matter Mater. Phys.* **1994**, *49*, 5554–5564.

(21) Krug, J. New mechanism for impurity-induced step bunching. *Europhys. Lett.* **2002**, *60*, 788.

(22) Sato, M. Effect of immobile impurities on motion of steps on a vicinal face. *Phys. Rev. E* **2011**, *84*, 061604.

(23) Ranganathan, M.; Weeks, J. D. Impurity effects in crystal growth from solutions: Steady states, transients and step bunch motion. *J. Cryst. Growth* **2014**, *393*, 35–41.

(24) Krzyzewski, F.; Zaluska-Kotur, M.; Krasteva, A.; Popova, H.; Tonchev, V. Step bunching and macrostep formation in 1d atomistic scale model of unstable vicinal crystal growth. *J. Cryst. Growth* **2017**, *474*, 135.

(25) Ranganathan, M.; Weeks, J. D. Theory of Impurity Induced Step Pinning and Recovery in Crystal Growth from Solutions. *Phys. Rev. Lett.* **2013**, *110*, 055503.

(26) Lutsko, J. F.; González-Segredo, N.; Durán-Olivencia, M. A.; Maes, D.; Van Driessche, A. E. S.; Sleutel, M. Crystal growth cessation revisited: The physical basis of step pinning. *Cryst. Growth Des.* **2014**, *14*, 6129–6134.

(27) Sleutel, M.; Lutsko, J. F.; Maes, D.; Van Driessche, A. E. S. Mesoscopic impurities expose a nucleation-limited regime of crystal growth. *Phys. Rev. Lett.* **2015**, *114*, 245501.

(28) Lutsko, J. F.; Van Driessche, A. E. S.; Durán-Olivencia, M. A.; Maes, D.; Sleutel, M. Step crowding effects dampen the stochasticity of crystal growth kinetics. *Phys. Rev. Lett.* **2016**, *116*, 015501.

(29) Khokhryakov, A. F.; Palyanov, Y. N.; Borzdov, Y. M.; Kozhukhov, A. S.; Shcheglov, D. V. *Cryst. Growth Des.* **2017**, *17*, DOI: 10.1021/acs.cgd.7b01025.